

Eigencurrent Expansion and Linear Embedding Via Green's Operators applied to design optimization of devices in Electromagnetic Band-Gap Structures

D. Duque, V. Lancellotti, B.P. de Hon, and A.G. Tijhuis

Department of Electrical Engineering, Eindhoven University of Technology
P.O. Box 513, 5600 MB, Eindhoven, the Netherlands
d.j.duque@tue.nl

Abstract

We present an efficient formulation based on the *linear embedding via Green's operators* (LEGO) and the *eigencurrent expansion method* to optimize composite wave interaction structures, e.g., photonic-crystal based devices. In LEGO, a composite structure is broken up into “bricks” that are characterized through *scattering operators* and the interaction among them is captured using *transfer operators*. By exploiting this *diakoptic* nature of LEGO, we show how the optimization is accomplished using an effective operator defined over the bricks (usually few) enclosing the space where the fields are sampled. This operator encompasses the effect of the surrounding and separates the domain to be optimized from the fixed one, enabling us to carry out the optimization with little computational effort.

1 Introduction

Over the past years, the interest in photonic crystals (PhC) has been driven by the ability to confine and guide energy by adding defects to the crystal. This characteristic has made PhCs essential components of photonic integrated circuits (PICs), and correspondingly, the need for *efficient* and *reliable* numeric modelling tools for such structures has increased. Commonly, simulations of PhC devices are performed using the finite difference time domain (FDTD) method [1, 2]. Although FDTD may provide a complete frequency characterization in a single run, it also has some drawbacks. First, the refinement of FDTD mesh will easily drain computational resources for electrically large structures. Second, if one wants to consider variations within a *small designated* domain in a design stage, FDTD would require a full rerun for the whole structure.

To address these issues, we apply electromagnetic modelling to a general PhC structure using the *linear embedding via Green's operators* with the *eigencurrent expansion method* (LEGO-EEM). LEGO is a domain decomposition method (DDM) where a composite structure is broken up into “bricks” that are characterized through *scattering operators*. To capture the interaction among the bricks, *transfer operators* are defined. To efficiently deal with large structures, we combine LEGO with the eigencurrent expansion method (EEM). In the EEM a set of basis functions that are good approximation to the true eigenfunctions of the relevant operator are used, resulting in a remarkable order reduction. We will show how with LEGO, any optimization can be performed by using an effective operator defined over the bricks (usually few) enclosing the space where the fields are sampled. This operator encompasses the effect of the surrounding and separates the domain to be optimized from the fixed one.

As an application example, we use LEGO-EEM to optimize a PhC-based channel drop filter (CDF) [2]. Briefly, in a CDF a propagating mode is transferred from one waveguide (called the *bus*) to another waveguide (called the *drop*) through a resonant element [1, 3, 4]. This paper is organized as follow: In section 2 we present a general formulation for optimization using LEGO-EEM. In section 3, we apply that formulation to optimize a typical CDF, and finally in section 4 conclusions are given.

2 An Efficient Formulation for Optimization using LEGO-EEM

Consider a structure composed of $N_B + N_T$ elements in a homogeneous background as shown in Figure 1. With N_B elements with “fixed” properties and N_T elements with composition and shape that are to be optimized. We refer to the latter as the “target” elements and we assume time-harmonic fields with $\exp(j\omega t)$ time dependency.

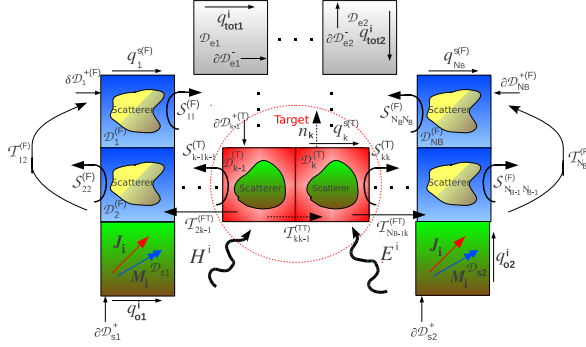


Figure 1: A structure is divided into bricks which are characterized by scattering operators \mathcal{S}_{kk} . The multiple scattering in the structure is captured by transfer operators \mathcal{T}_{kn} . A portion of the structure is identified as the “target” in the optimization.

We embed each element in a bounded domain \mathcal{D}_k , $k = 1, \dots, N_B + N_T$, dubbed brick, which we characterize through a *scattering operator* \mathcal{S}_{kk} [5]. The region where the fields are to be sampled is also embedded in bricks \mathcal{D}_{el} with boundary $\partial\mathcal{D}_{el}$, $l = 1, \dots, N_e$; we refer to them as the “empty” structure. In a similar fashion, the sources are embedded in bricks \mathcal{D}_{sj} , $j = 1, \dots, N_s$ forming the “source” domain. We seek for an expression of the *total equivalent incident current* $\mathbf{q}_{\text{tot}}^i = [\mathbf{J}_{\text{tot}}^i \mathbf{M}_{\text{tot}}^i]^t$ on $\partial\mathcal{D}_{el}^-$ that in the light of Love’s equivalence principle reproduces the actual field in \mathcal{D}_{el} . We similarly define an *outer equivalent incident current* $\mathbf{q}_{on}^i = [\mathbf{J}_{on}^i \mathbf{M}_{on}^i]^t$ on $\partial\mathcal{D}_{sn}^+$, $n = 1, \dots, N_s$ that reproduces the field radiated by the sources (see Figure1). These currents are related by

$$\mathbf{q}_{\text{tot}}^i = \mathbf{q}^i + \mathcal{T}^{(eF)} \mathbf{q}^{s(F)} + \mathcal{T}^{(eT)} \mathbf{q}^{s(T)}, \quad (1)$$

$$\begin{bmatrix} \mathcal{S}^{-1(F)} & -\mathcal{T}^{(FT)} \\ -\mathcal{T}^{(TF)} & \mathcal{S}^{-1(T)} \end{bmatrix} \begin{bmatrix} \mathbf{q}^{s(F)} \\ \mathbf{q}^{s(T)} \end{bmatrix} = \begin{bmatrix} \mathcal{T}^{(FS)} \\ \mathcal{T}^{(TS)} \end{bmatrix} [\mathbf{q}_o^i], \quad (2)$$

where $\mathbf{q}_{\text{tot}}^i = [q_{\text{tot}1}^i, \dots, q_{\text{tot}N_e}^i]^t$, $\mathbf{q}_o^i = [q_{o1}^i, \dots, q_{oN_s}^i]^t$, $\mathbf{q}^i = [q_1^i, \dots, q_{N_c}^i]^t$ is the *equivalent incident current* on the empty structure, $\mathbf{q}^{s(F)} = [q_1^{s(F)}, \dots, q_{N_B}^{s(F)}]^t$ is the *equivalent scattered current* on the fixed structure, $\mathbf{q}^{s(T)} = [q_1^{s(T)}, \dots, q_{N_T}^{s(T)}]^t$ is the *equivalent scattered current* on the target, and any \mathcal{T} and \mathcal{S}^{-1} are *current transfer operators* and a *inverse scattering operators* respectively [5]. We efficiently solve (1)-(2) using the MoM with the EEM [5]. Thereby, the algebraic counterpart of (2) becomes

$$\begin{bmatrix} [\check{\mathcal{S}}_{cc}^{(F)}]^{-1} & -[\check{\mathcal{T}}_{cc}^{(FT)}] \\ -[\check{\mathcal{T}}_{cc}^{(TF)}] & [\check{\mathcal{S}}_{cc}^{(T)}]^{-1} \end{bmatrix} \begin{bmatrix} [\check{\mathbf{q}}_c^{s(F)}] \\ [\check{\mathbf{q}}_c^{s(T)}] \end{bmatrix} = \begin{bmatrix} [\check{\mathcal{T}}_c^{(FS)}] \\ [\check{\mathcal{T}}_c^{(TS)}] \end{bmatrix} [\mathbf{q}_o^i], \quad (3)$$

$$[\check{\mathbf{q}}_u^{s(F)}] = [\check{\Lambda}_{uu}^{(F)}] [\check{\mathcal{T}}_u^{(FS)}] [\mathbf{q}_o^i], [\check{\mathbf{q}}_u^{s(T)}] = [\check{\mathcal{S}}_{uu}^{(T)}] [\check{\mathcal{T}}_u^{(TS)}] [\mathbf{q}_o^i], \quad (4)$$

where we have used the check accent to indicate that (3) is the algebraic counterpart of (2) in the $N_c \times (N_B + N_T)$ *coupled* eigencurrent basis and (4) represents the same in the $N_u \times (N_B + N_T)$ *uncoupled* eigencurrent basis. Here, $[\check{\mathcal{S}}_{uu}^{(T)}] = \text{diag} \{ [\check{\mathcal{S}}_{uu,kk}^{(T)}] \}$ i.e. a block diagonal matrix containing the uncoupled entries of $[\check{\mathcal{S}}_{kk}^{(T)}]$. Note that in (3) and (4) we keep $[\mathbf{q}_o^i]$ in the original basis. By defining $[\check{\Sigma}_{cc}^{(T)}] = [\check{\mathcal{S}}_{cc}^{(T)}]^{-1} - [\check{\mathcal{S}}_{cc}^{(F)}]$, $[\check{B}_c^{(TS)}] = [\check{\mathcal{T}}_{cc}^{(TF)}] [\check{\mathcal{S}}_{cc}^{(F)}] [\check{\mathcal{T}}_c^{(FS)}]$ and $[\check{\mathcal{S}}_{cc}^{(T/F)}] = [\check{\mathcal{T}}_{cc}^{(TF)}] [\check{\mathcal{S}}_{cc}^{(F)}] [\check{\mathcal{T}}_{cc}^{(FT)}]$ as the *scattering matrix* of the fixed structure as seen from the target, we obtain

$$\begin{aligned} [\mathbf{q}_{\text{tot}}^i] &= [\mathbf{q}^i] + [\check{\mathcal{T}}_u^{(eF)}] [\check{\Lambda}_{uu}^{(F)}] [\check{\mathcal{T}}_u^{(FS)}] [\mathbf{q}_o^i] + [\check{\mathcal{T}}_u^{(eT)}] [\check{\mathcal{S}}_{uu}^{(T)}] [\check{\mathcal{T}}_u^{(TS)}] [\mathbf{q}_o^i] + [\check{\mathcal{T}}_c^{(eF)}] [\check{\mathcal{S}}_{cc}^{(F)}] [\check{\mathcal{T}}_c^{(FS)}] [\mathbf{q}_o^i] \\ &+ [\check{\mathcal{T}}_c^{(eT)}] [\check{\Sigma}_{cc}^{(T)}]^{-1} \left([\check{\mathcal{T}}_c^{(TS)}] + [\check{B}_c^{(TS)}] \right) [\mathbf{q}_o^i] + [\check{\mathcal{T}}_c^{(eF)}] [\check{\mathcal{S}}_{cc}^{(F)}] [\check{\mathcal{T}}_{cc}^{(FT)}] [\check{\Sigma}_{cc}^{(T)}]^{-1} \left([\check{\mathcal{T}}_c^{(TS)}] + [\check{B}_c^{(TS)}] \right) [\mathbf{q}_o^i]. \end{aligned} \quad (5)$$

We observe that in (5) only $[\check{\mathcal{S}}_{cc}^{(T)}]$ and $[\check{\mathcal{S}}_{uu}^{(T)}]$ have to be updated by recomputing $[\check{\mathcal{S}}_{kk}^{(T)}]$ when a parameter in the target changes, the other matrices are constant as long as the eigencurrent basis is fixed. This feature renders (5) an *efficient* formulation for optimization, since enables to tune the target with little computational effort. Moreover in general $N_c \ll 2N_f$ with $N_c + N_u = 2N_f$ i.e. the number of basis functions used to expand $q_k^{s(F,T)}$ on $\partial\mathcal{D}_k^\pm$, thereby, a significant amount of memory is saved when storing the matrices in (5).

3 LEGO and EEM applied to the Design of Photonic-Crystal based Channel Drop Filters

We realize the CDF using an array of 2-D dielectric posts with radius $r = 0.2a$ and $\varepsilon_r = 11.56$ that have been embedded in as much square bricks as Figure 2 shows. This array of posts exhibits a large TMz band-gap with $fa/c \in [0.29, 0.42]$ [2], with c the speed of light and a the lattice constant. Note that for the cavity posts we have taken the fixed parameters as in [2]. Hence, the cavities are made by reducing two post radius to $r = 0.05a$ and their permittivity to $\varepsilon_r = 6.60$. It is expected that these cavities exhibit a single monopole mode at resonance. A frequency sweep has shown this resonance to be at $f_0 a/c \approx 0.372$. If there are no losses in the waveguides and the cavities, it is not difficult to find using couple mode theory [4] that the maximum of $\frac{|V_6^-|^2}{|V_1^+|^2}$ in Figure 2 occurs when the *symmetric* mode $a_s = \frac{a_1 + a_2}{\sqrt{2}}$ and the *antisymmetric* mode $a_{\bar{s}} = \frac{a_1 - a_2}{\sqrt{2}}$ at the cross-section, are degenerate at the resonant frequency of one single cavity [1, 2]. This is mathematically stated as

$$C - 2|k|^2 \sin \beta d = 0, \quad (6)$$

where k is the coupling constants waveguide-cavity, β is the propagation constant in both waveguides and jC as the cavity-cavity coupling constant with $C \in \mathbb{R}$ [2]. According to (6) the *direct* cavity-cavity coupling and the *weak indirect* waveguide-cavity coupling must be balanced. We proceed by applying our full-wave optimization strategy using (5) to effectively accomplish (6). In our optimization procedure, we regard (6) as an equality constraint for the fixed resonance frequency. In Figure 2 we set $\beta d = \frac{\pi}{2} + m\pi$ with $m = 2$ thus $d = 5a$ since simulations show that $\beta \approx 0.25 \cdot 2\pi/a$. The two parallel waveguides are made by removing two row of posts and they will be ended by matching terminations. Before we describe the optimization of the target bricks in Figure 2, we consider the matching termination.

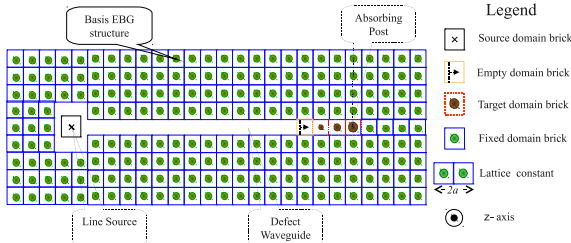


Figure 3: Setup for the optimization of the absorbing posts.

Figure 2 shows the minimization of CF_2 with initial guess of $\varepsilon_r = 9.50$, $\mu_r = 1.0$ and $r = 0.2a$ using the subroutine E04JYF of the NAG library. The found permittivity and radius for the target posts are $\varepsilon_r \approx 3.42$, $\mu_r = 1.0$

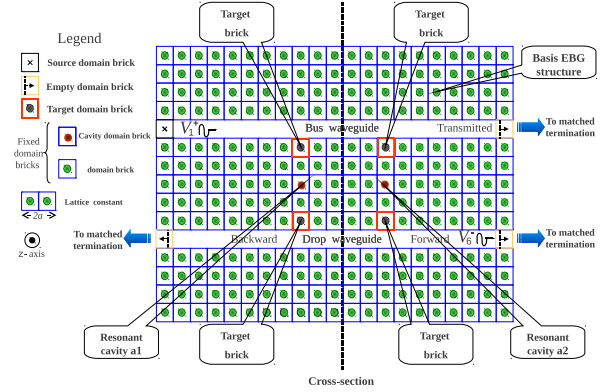
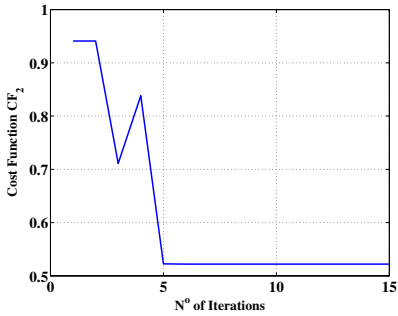


Figure 2: CDF with two equal single mode cavities and parallel waveguides. Matching terminations are used to suppress reflected incoming signals.

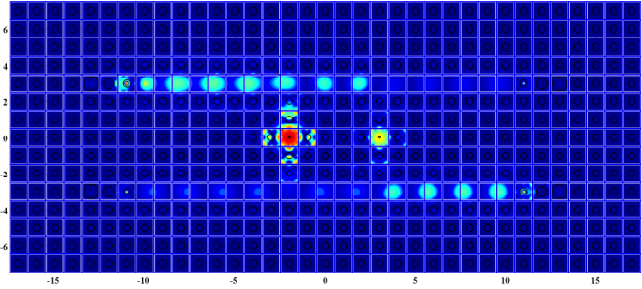
The matching termination consists of three *absorbing* posts with radius $r_1 = 0.2a$, $r_2 = 0.3a$, $r_3 = 0.4a$ and $\varepsilon_{r1} = \mu_{r1} \approx 9.74 - j0.00$, $\varepsilon_{r2} = \mu_{r2} \approx 19.34 - j34.72$ and $\varepsilon_{r3} = \mu_{r3} \approx 4.68 - j0.00$ that have been optimized using (5) in the setup of Figure 3, where again the source and all the posts have been embedded in square bricks. The rationale was to maximize the normal component of the *Poynting* vector (with respect to the cross-section) at resonance in an empty brick in the defect waveguide, thus minimizing the reflected power. The cost function was defined as $CF_1 = |\mathcal{S}_n^0|/|\mathcal{S}_n^i|$ where $|\mathcal{S}_n^0|$ is the normal *Poynting* vector in the empty brick when the defect waveguide is open to background i.e. all posts to the right of the empty brick and along the waveguide are removed and $|\mathcal{S}_n^i|$ is the normal *Poynting* vector at iteration i . We do not include the detailed results of this optimization for sake of brevity.

We now proceed to accomplish (6) by playing with the waveguide-cavity coupling constant in Figure 2. Thereby, we use four alike posts with unknown ε_r and radius as the target in order to maximize the transferred power in the *forward* direction while minimizing the *transmitted* power and the transferred power in the *backward* direction. Hence, the cost function is defined as $CF_2 = P_t/P_s + P_b/P_s + (1 - P_t/P_s)$ where P_t is the transmitted power, P_b is the transferred power in the backward direction, P_f is the transferred power in the forward direction and P_s is the power delivered by the source which is computed using the currents on the brick that embeds the source. To sense these powers we have considered three sampling bricks in the waveguides. To excite the CDF a current line source is used and once again (5) will be the *core* engine to minimize the cost function. To perform this optimization, we use $2N_f = 104$ triangle basis functions to expand any equivalent current on each brick, we retain $N_c^{(F)} = 21$ and $N_u^{(F)} = 83$ basis functions, while for the target we have $N_c^{(T)} = 100$ and $N_u^{(T)} = 4$.

Figure 4(a) shows the minimization of CF_2 with initial guess of $\varepsilon_r = 9.50$, $\mu_r = 1.0$ and $r = 0.2a$ using the subroutine E04JYF of the NAG library. The found permittivity and radius for the target posts are $\varepsilon_r \approx 3.42$, $\mu_r = 1.0$



(a) The cost function CF_2 vs N° of iterations



(b) Field distribution $|E_z|$ showing the tunneling effect in the CDF after optimization.

Figure 4: Optimization results for the simulated CDF

and $r \approx 0.173a$ and the power ratios amount to $\frac{P_t}{P_s} \approx 0.116$, $\frac{P_b}{P_s} \approx 0.109$ and $\frac{P_r}{P_s} \approx 0.703$ for an estimated transfer efficiency of 70.3%. Figure 4(b) shows a snapshot of $|E_z|$ showing the cavity tunneling effect.

Table 1: Characteristic sizes and memory usage (MB)

Channel Drop Filter optimization		
$N_B = 479, N_T = 4, 2N_f = 104, N_c^{(F)} = 21, N_c^{(T)} = 100$		
	LEGO-EEM	(BIE)
$[\tilde{T}_{cc}^{(TF)}]$	400×10059 (61)	416×49816 (316)
$[\tilde{T}_c^{(eF)}]$	312×10059 (48)	312×49816 (237)
$[\tilde{S}_{cc}^{(F)}]$	10059×10059 (1.5 GB)	49816×49816 (37 GB)

Table 1 summarizes the memory usage for the dominant matrices in (5) when using a boundary integral equation (BIE) directly posed on the cylinder contours and LEGO-EEM. The advantage of (5) to handle large structure is remarkable judging by the achieved average compression ratio of $\bar{c}_r = 84.5\%$ in memory usage.

4 Conclusions

We have endowed LEGO with the EEM to efficiently tackle large electromagnetic problems. We have seen that LEGO-EEM efficiently allows for fine tuning of a target domain by only recomputing the scattering matrices of the bricks whose content changes. We have applied the presented formulation in a typical CDF configuration and we have achieved *good* tunneling in few iterations though not 100% as the simplified model predicts. Nevertheless, LEGO-EEM has proved to be an exceptional tool for optimization.

Acknowledgments

This research was supported by the MEMPHIS project under contract No 10006758.

References

- [1] S. Fan, P.R. Villeneuve, J.D. Joannopoulos, and H.A. Haus, "Channel drop filters in photonic crystals," *Optic Express* 4, 1998.
- [2] S. Fan, P. R. Villeneuve, J.D. Joannopoulos, M.J.Khan, C.Manolatou, and H.A.Haus, "Theoretical analysis of channel drop tunneling processes," *Physical Review B*, 1999.
- [3] S. Fan, P. R. Villeneuve, J.D. Joannopoulos, and H.A Haus, "Channel drop tunneling through localized states," *Physical Review Letter*, 1998.
- [4] C.Manolatou, M.J. Khan, S. Fan, P. R. Villeneuve, H.A Haus, and J.D. Joannopoulos, "Coupling of modes analysis of resonant channel add-drop filters," *IEEE J. Quantum Electron.*, 1999.
- [5] V.Lancellotti, B.P. de Hon, and A.G.Tijhuis, "An eigencurrent approach to the analysis of electrically large 3-D structures using LEGO," *IEEE Trans. Antennas Propagat.*, vol. 57, pp. 3575–3585, Nov. 2009.